Dislocation-based model of crack-tip shielding effects

J. Pokluda
Institute of Physical Engineering, Brno University of Technology, Brno, (Czech Republic)
pokluda@fme.vutbr.cz

ABSTRACT. Along with external forces and the macro-geometry of cracked bodies, the local stress intensity factors k (or Δk) at fronts of brittle and fatigue cracks are also determined by internal residual stress fields and the crack front microgeometry (extrinsic shielding). Consequently, the values of k (Δk) that represent a real crack driving force can be significantly different from those of the remote K (ΔK). This means that, even in the frame of linear-elastic fracture mechanics, a characterization of the crack-tip stress field by a single K (ΔK) parameter is not sufficient.
The paper presents a discrete dislocation model of extrinsic crack-tip shielding effects that appear in fatigue due to small-scale yielding. The main advantages of this multi-scale model with respect to LEFM models based on continuum mechanics are its simplicity and physical transparency. This enables us to directly asses the magnitude of both plasticity and roughness-induced components of crack closure which is not possible by means of multi-parameter continuum LEFM models of the crack-tip stress field. Also beyond the frame of continuum models, the dislocation model includes a physically justified parameter expressing an influence of microstructure on the roughness-induced shielding term. Based on the analytical formula and standard materials data on mechanical properties and microstructure, the closure components can be simply extracted from experimentally measured values of ΔK which is not possible by experimental crack-closure measurements. In this way, the effective threshold $\Delta K_{th,eff}$ can be obtained as nearly independent of microstructure coarseness and applied cyclic ratio. The practical importance of the dislocation-based model is documented by the fact that the threshold ΔK_{th} is a basic material characteristic used in predictions of fatigue strength and life of cracked components.

KEYWORDS. Crack-tip shielding, discrete dislocations, multi-parameter description, fatigue crack-growth, plane strain, effective threshold, size ratio, microstructure distance.

INTRODUCTION

The crack driving force in fatigue is, unlike in brittle fracture, directly related to the range of the cyclic plastic strain at the crack tip [1]. Because the maximum K-value during the stable crack growth lies below the critical stress intensity factor (SIF) K_c, the crack growth can proceed only when supported by the work of external cyclic forces. In 1963, Paris and Erdogan [2] proved that the diagram da/dN vs ΔK for so-called long cracks in the small-scale yielding range (high-cycle fatigue) retains the advantage of LEFM, namely a satisfactory invariance in the shape and size of cracked solids. It might seem to be surprising that the linear-elastic parameter also allows us to describe successfully the rate of plastic processes at the crack tip. Several years later, however, Rice [3] brought to light a theoretical reason justifying the present opinion: the small-scale cyclic plasticity (the cyclic plastic zone) at the crack tip is, indeed, controlled by the value of ΔK. This gives us a further good reason why to describe the stress field ahead of fatigue cracks in terms of LEFM parameters.

The real value of ΔK at the crack tip is determined by both external and internal stresses resulting from external forces and local plastic deformations (or generally from microstructural defects), respectively. In fatigue, the level of internal stresses can substantially influence the stable growth rate, since the emission of dislocations from the crack tip occurs at very low stress intensity factors. This means that even very small changes of local k-values at the crack tip can considerably modify the stable crack growth rate. Thus, the internal stresses created by dislocation configurations and secondary phases are to be considered as an important additional factor affecting the fatigue crack propagation rate. It is particularly this difference that elucidates a much higher complexity of shielding (or anti-shielding) effects accompanying the fatigue crack growth when compared to brittle fracture. For example, the contact shielding (crack closure) in fatigue also occurs under the opening mode I which is not the case of unstable cracks under monotonic loading.

Most of the extrinsic crack-tip shielding effects in fatigue are a consequence of the plastic zone around the crack front and along the crack flanks. During the last years, many attempts have been made to incorporate the shielding effects (particularly crack closure) into the LEFM description of the crack-tip stress field, e.g., [4 - 6]. These models represent multi-parameter approaches based on the continuum mechanics. On the other hand, there are several models based on discrete dislocation approaches that were developed rather recently, e.g., [1, 7 - 9]. *The main advantage of these dislocation-based models in comparison with multi-parameter continuum ones is their physical transparency which enables us to quantitatively assess both the plasticity-induced and roughness-induced crack closure (PICC and RICC) components using standard materials data. These models also include a physically justified parameter expressing an influence of microstructure on the RICC term which is not reflected in multi-parameter continuum models.*

Extrinsic shielding caused by the geometrical tortuosity of the crack front (so-called geometrical shielding) will not be discussed here since it can be neglected in most metallic materials [1, 10]. Effect of the T-stress on fracture toughness and fatigue resistance will also be omitted since it is not induced by the local plasticity. Nevertheless, the sign and value of this parameter have some influence on the resistance to crack growth by inhibiting (shielding) or raising (antishielding) the dislocation emission from the crack tip.

The main aim of this paper is to briefly describe the basic principles of the discrete dislocation model and to show its capability to assess the contact shielding terms and to separate them from the measured remote ΔK values. In this way, the effective threshold $\Delta K_{th,eff}$ can be determined without performing complicated and not too much reliable crack closure measurements. We will mainly focus on the plane-strain case which is more important from the engineering point of view.

PRINCIPLES OF DISLOCATION MODELS IN PLANE STRESS AND PLANE STRAIN

Fatigue cracks propagate owing to a partly irreversible dislocation emission and absorption processes that produce quasi-periodical arrays of dislocations ahead of the crack front and in the crack wake [1, 11, 12]. In this way, a "static" plastic zone is always formed by both the geometrically necessary and the statistically stored dislocations ahead of the crack tip and around the crack flanks.

Plane stress

A simplified picture of these dislocation arrays can be seen in Fig. 1 where only the geometrically necessary edge dislocations are depicted. Many of these dislocations are moving along slip planes that intersect the crack plane along the whole crack front and produce a "longitudinal" necking of the plastic zone in the crack wake (visible at the crack mouth on the free surface) in the x-direction. This necking is produced by a tilting of the crystal lattice generated by dislocation bands (low-angle tilt boundaries) left in the crack wake. In thin specimens (plane stress), a "transversal" necking inside the plastic zone in the z-direction can also be produced by dislocations (marked by circles) that move in oblique planes which intersect the crack front in just one point. The dislocation array produces a long-range stress field that induces both PICC and RICC. This field is an analogy to the shielding stress field (shielding forces) for an unloaded crack in the frame of the multi-parameter continuum model as shown in Fig. 2 [6]. The surrounding elastic material exerts the compressive force F_{py} (constraining the plastic stretching) and the tensile force F_{px} (obstructing the plastic contraction) on the plastic zone. When such a constrained plastic zone transfers from the crack front to the crack wake due to the crack advance, these forces (stresses) are gradually released. As a consequence, the plastic elements stretch in the direction perpendicular to the crack plane (y-direction) to form a plastic wedge between the crack flanks. This wedge is the main reason for a premature contact of crack flanks (PICC) in the plane stress case. The related closing force F_c is marked in the crack wake in Fig. 2. Previous analytical and numerical models assessed the value of the residual stretch to be close to the crack tip opening displacement $\delta_t \approx K^2/(\sigma_y E)$ under small-scale yielding conditions [13]. This leads, in agreement with experiments, to the closure ratio $K_{cl}/K_{max} \approx 0.5$ with a moderate dependence of the cyclic ratio.

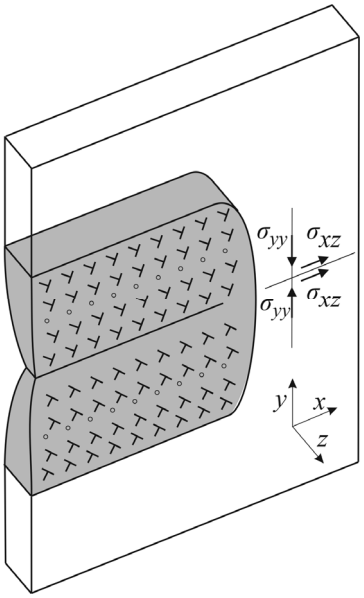

Figure 1: Dislocation arrays forming the plastic zone in the plane stress case.

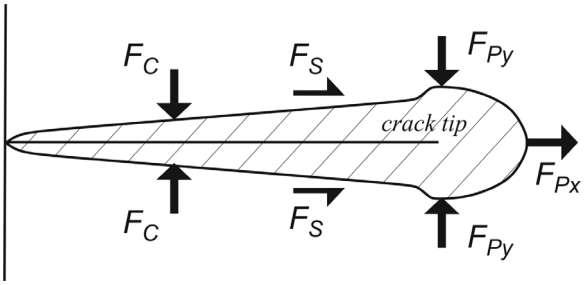

Figure 2: Shielding forces considered in continuum multi-parameter model [6]. The hatching marks the plastic region around the crack.

The longitudinal necking causes a transfer of mass along the crack flanks towards the crack front. This results in a mass surplus at the crack front which contributes to the crack closure effect. Indeed, the crack-wake dislocation bands produce a stress consisting of closure and shear components σ_{yy} and σ_{xz} near the crack tip as depicted in Fig. 1. The stress σ_{yy} contributes to both forces F_{py} and F_c whereas σ_{xz} is an analogy to the force F_S directed along the elastic-plastic boundary in the continuum multi-parameter model (see Fig. 2). The closure component σ_{yy} is associated with the local shielding factor k_1 (mode I) whereas the shear component σ_{xz} with the factor k_2 (mode II) that can produce RICC as discussed hereafter in more details.

Owing to a rather complicated dislocation structure of the plane stress model, the assessment of PICC and RICC components was not performed hitherto. It should be noted, however, that the description of shielding effects in terms of SIFs under the plane-stress conditions is only of a very restricted practical importance. Indeed, the plane-stress cracks usually exhibit *R*-curve behaviour and, moreover, the plane-strain conditions prevail in most of cracked samples and components particularly in the near-threshold crack growth region.

Plane strain

In the more important case of plane strain, the PICC can also be detected, albeit to a much lower extent: the closure ratio $K_{cl}/K_{max} \approx 0.2 – 0.25$ [1, 14, 15]. A certain level of RICC can also be produced. These effects are mainly a consequence of the closing stress σ_{yy} (the factor k_1) and the stress σ_{xz} (the factor k_2) related to the longitudinal contraction. The transverse contraction along the crack front is not allowed by definition and, therefore, the plastic wedge in the crack wake is significantly reduced in comparison to the plane strain case. The shear stress σ_{xz} and the related shear displacement u_2 (see

eq. (2)) are of a long-range character: they approach a constant value along the crack flanks [7]. On the other hand, the compressive stress σ_{yy} and the related displacements u_1 causing an "overlapping" of crack flanks become maximal at the crack tip and already disappear at distances about several microns from the crack tip. Therefore, the PICC takes place only at a rather close vicinity of the crack tip. This behavior is, besides the closure level, the main difference between the PICC under plane strain and plane stress conditions. In the latter case, indeed, the plastic wedge causes an extensive PICC along a substantial part of the crack flanks.

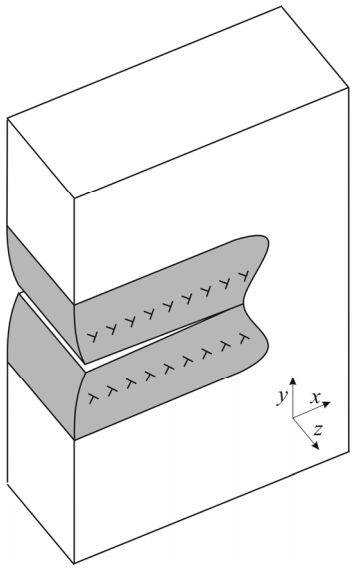

Figure 3: Single dislocation strips replacing the real array under plane strain conditions.

An integration performed over many dislocation bands of the real dislocation array allows us to replace this array just by a single strip of an effective dislocation density. This is schematically shown in Fig. 3 which also reflects a much less extent of the plastic zone in comparison to the plane-stress case (for an equal applied SIF).

ASSESSMENT OF CRACK CLOSURE COMPONENTS UNDER PLANE STRAIN CONDITIONS

Plasticity-induced crack closure

Each dislocation strip in the scheme in Fig. 3 produces the local shielding stress intensity factors k_1 and k_2 near the crack tip as

$$\begin{pmatrix} k_1 \\ k_2 \end{pmatrix} = Gb\sqrt{r}\,\frac{1}{D}\begin{pmatrix} c_1 \\ c_2 \end{pmatrix} \tag{1}$$

where r is the distance of a single band of dislocations from the crack flanks, D is the effective spacing between individual dislocations in the array and c_I and c_{II} are constants of about -1 [1, 7]. In the near tip regime, the displacements at the crack read

$$\begin{pmatrix} u_1 \\ u_2 \end{pmatrix} = \frac{2(1-\nu)}{G}\sqrt{\frac{|x_c|}{2\pi}}\begin{pmatrix} k_1 \\ k_2 \end{pmatrix} \tag{2}$$

where x_c is the distance of the crack-wake contact of crack flanks from the crack tip (units of μm). Note that an overlap of the crack flanks near the crack tip takes place (k_1 and u_1 are negative). When assuming that dislocation strips on both sides of the crack flanks contribute to PICC, the following simple relation for the closure ratio can be derived:

$$K_{cl,p}/K_{max} = 2C \tag{3}$$

where $C \approx 0.1$ is a dimensionless constant nearly independent of the material (see, e.g., [1] for more details). This result agrees well with experimentally determined PICC values under plane strain.

Maximal roughness-induced crack closure

When the crack flanks are rough and the arrangement of crack-wake dislocations becomes asymmetric the shear displacements of both crack flanks are different. This shear misfit causes the long-range RICC on rough fracture surfaces as depicted for an extremely asymmetric dislocation arrangement in Fig. 4. Such arrangements can produce RICC far behind the crack tip, in contrast to shear displacements induced by the short-range RICC (see hereafter). Thus, both the asymmetry of crack-wake dislocations and the roughness of fracture surfaces can be assumed to be the necessary conditions for the appearance of long-range RICC.

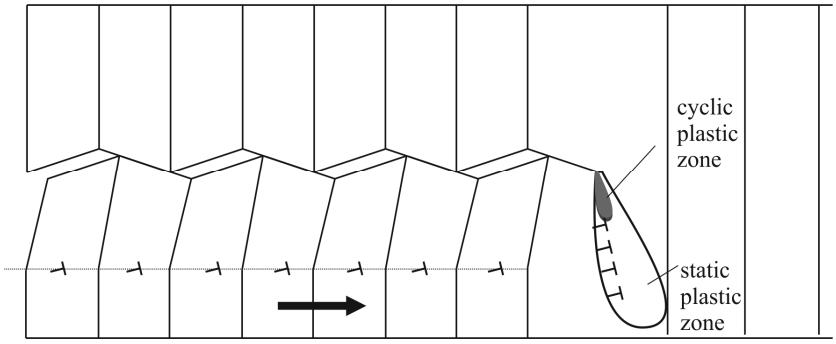

Figure 4: Scheme of the asymmetric dislocation array inducing the maximal long-range roughness-induced crack closure.

The maximum possible level of RICC can be determined by considering a single dislocation strip that produces the local SIF k_2 and the crack-flank shear displacement u_2 according to eqs. (1) and (2), respectively. Assuming simple (zigzag) roughness geometry, the maximal long-term RICC ratio reads

$$\frac{K_{d,rl}}{K_{max}} = C\sqrt{\left(R_A^2 - 1\right)} \tag{4}$$

where R_A is the area roughness of crack flanks [9].

The short-range RICC component is associated with the local mode II induced by the zigzag crack path and it is created by an irreversible slip at the crack tip (see [1, 16] for more details). The related maximal closure ratio can be assessed as

$$\frac{K_{d,rs}}{K_{max}} = \frac{3\left(R_A - 1\right)}{2\sqrt{6} + 6\left(R_A - 1\right)} \tag{5}$$

Size ratio effect

A lot of experimental evidence about the special role of the mean size ratio $S_{Rm} = d_m/r_p$, where d_m is the mean value of the characteristic microstructural distance d (grain size or interparticle spacing) and r_p is the static plastic zone size, was collected during the last three decades of experimental and theoretical fracture and fatigue research, e.g., [17-19]. Numerous experiments revealed that the crack path is particularly influenced by microstructure (grain boundaries, phase boundaries, precipitates, inclusions) when $S_{Rm} \geq 1$. The above mentioned necessary conditions for RICC are well fulfilled exactly when $S_{Rm} \geq 1$. In this case, the static plastic zone is constrained within individual grains containing the crack front. The grain boundaries or secondary phase particles constitute obstacles for crack growth which leads to microscopically rough crack flanks and a highly asymmetric crack-wake plasticity (see, e.g., [1, 9] for more details). In the case of $S_{Rm} < 1$, the plastic zone embraces several grains or particles and the grain boundaries and the secondary phases do not constitute obstacles for the crack growth. Consequently, the plastic zone is not restricted by microstructural barriers on either side of the crack flanks and there is no reason for the asymmetry of the crack-wake plasticity. Let us emphasize that the size ratio effect is not so significant for PICC since the dislocation bands on both sides of the crack flanks contribute to this closure effect.

In most engineering materials, the scatter of both the grain size and the particle spacing causes variation of the parameter d within more than two orders of magnitude along the crack front. On the other hand, a sharp decrease of the stress with distance from the crack front leads to localization of the plastic deformation within a narrow plastic zone of approximately constant width along the whole crack front. As a consequence, the size ratio $S_R = d/r_p$ follows the Weibull grain size distribution and varies in a wide range along the crack front inside the specimen which means that many sites at

both the crack front and crack flanks where $S_R < 1$ or $S_R \geq 1$ are to be expected. However, only the latter locations contribute to the RICC while the effect of the former ones can be neglected. The basic idea of the statistical approach introduced in [16] lies in an assumption that the microstructure elements can be divided into two main categories of low and high S_R. This means that the low S_R part of the probability density function does not influence the RICC that is controlled by the high S_R part. The probability of finding an element with $S_R \geq 1$ at the crack tip (or flanks) can be expressed as

$$\eta = \left[-\left(\frac{0.866 S_{Rc} r_p}{d_m} \right)^{2.2} \right] \tag{6}$$

where $S_{Rc} \in (0.2; 1)$ determines the boundary between both categories of microstructural elements and r_p can be estimated on the basis of σ_y and K_{max}.. Although S_{Rc} remains the only fitting parameter in the model, the value $S_{Rc} \approx 0.5$ is usually well acceptable [1]. In order to determine the real level of RICC, the statistical size ratio effect must be taken into account. Consequently, both maximal closure ratios given by Eqs. (4) and (5) must be multiplied by the statistical parameter η.

EFFECTIVE STRESS INTENSITY RANGE

The total crack closure ratio represents a sum of PICC and RICC components given by Eqs. (3), (4) and (5). Considering $\Delta K_{eff} = K_{max} - K_{cl}$, $K_{max} = \Delta K/(1 - R)$ and the statistical size ratio effect, the effective SIF range reads

$$\Delta K_{eff} = \left(1 - C\eta\sqrt{R_A^2 - 1} - \frac{3\eta(R_A - 1)}{2\sqrt{6} + 6(R_A - 1)} - 2C \right) \frac{\Delta K}{1 - R} \tag{7}$$

Eq. (7) correctly reflects many interesting phenomena that were experimentally detected:

1. Both terms of the RICC must approach zero for microscopically straight (planar) cracks. This obviously corresponds to $R_A = 0$ and the contact shielding reduces only to the PICC term.
2. The total RICC level must also approach zero in the near fracture region of fatigue crack growth since the mean size ratio $S_{Rm} \rightarrow 0$ and $\eta \rightarrow 0$. Thus, the crack closure effect is also determined only by PICC.
3. The maximal level of RICC and the minimum of $\Delta K_{eff}/\Delta K$ ratio are detected in the near-threshold region, where, obviously, $S_{Rm} \gg 1$ and $\eta \rightarrow 1$ is to be expected.
4. For $R < 0.6$, the value of $\Delta K_{eff}/\Delta K$ decreases with decreasing cyclic ratio R, increasing area roughness R_A and decreasing plastic zone size (increasing η).

Eq. (7) also predicts that, in nanomaterials, the RICC level must be negligible in the whole fatigue crack growth region (not only near fracture). Indeed, the value of the effective threshold $\Delta K_{eff,th}$ is generally lower than 3 MPam$^{1/2}$ (see Tab. 1). Assuming $K_{max,th} \approx 5$ MPam$^{1/2}$ as a minimum value for $R < 0.6$ and considering $\sigma_y \approx 1000$MPa, one obtains $r_p \approx 2500$ nm in the near-threshold region. For nanomaterials with $d_m < 100$ nm it means that $S_{Rm} < 0.04$, $\eta \rightarrow 0$ and RICC $\rightarrow 0$. In these materials, consequently, a negligible level of RICC applies even to the near-threshold region and the threshold ΔK_{th} is relatively low. Recent experimental results [20] confirmed this conclusion.

Eq. (7) can be simply applied to the assessment of the effective thresholds and the closure components in engineering metallic materials since. Only a few standard material characteristics and loading parameters are necessary: σ_y, d_m, R_A, ΔK_{th} and R. The results of the $\Delta K_{eff,th}$ assessment for several metallic materials are collected in Tab. 1. For each material, a wide range of mean characteristic microstructure parameters and loading ratios was investigated. In most cases, the statistical parameter $\eta \approx 0.5$ was utilized in the calculations. Obtained values of $\Delta K_{eff,th}$ are well comparable to experimental data [21-26] and the related very small values of standard deviation reveal that they are, unlike the ΔK_{th} values, almost independent of microstructure and cyclic ratio.

	ARMCO iron	Austenitic steel	Titanium	Aluminium alloy (air)	Aluminium alloy (vacuum)
ΔK_{th}	6.0 ±2.4	3.1 ± 0.4	6.2 ± 1.7	2.3 ± 0.4	4.9 ± 2.3
$\Delta K_{eff,th}$	2.8 ±0.4	2.3 ± 0.2	2.6 ± 0.4	1.0 ± 0.1	1.8 ± 0.2

Table 1: Experimental thresholds ΔK_{th} and calculated effective thresholds $\Delta K_{eff,th}$ for various metallic materials.

Thus, the dislocation-based approach has the following advantages when compared to the continuum-based model:

- *physical transparency;*
- *quantitative assessment of both PICC and RICC components using standard materials data;*
- *incorporated influence of microstructure on RICC.*

The main practical importance of the relation at Eq. (7) lies in a possibility of its direct application to experimental data on ΔK and ΔK_{th} to calculate ΔK_{eff} and $\Delta K_{eff,th}$, respectively. Moreover, a clear physical background of RICC and PICC components offers an efficient tool to materials technologists for an improvement of the resistance to fatigue crack propagation by means of microstructure variation. It should be also noted that the threshold ΔK_{th} is a basic material characteristic used in predictions of strength and fatigue life of cracked components.

CONCLUSION

Dislocation-based model of contact shielding effects in fatigue was described and qualitatively compared to the recently published, continuum-based multi-parameter model. The main results of this study can be briefly summarized as follows:

1. There is a good qualitative agreement between the plasticity-induced shielding terms employed in dislocation-based and continuum-based multi-parameter models.
2. The main advantages of the dislocation-based model are the physical transparency, the possibility of direct quantitative assessment of both the plasticity-induced and the roughness-induced crack closure components and the incorporation of microstructure influence on the level of contact shielding.
3. Effective thresholds $\Delta K_{eff,th}$ calculated by application of the dislocation-based model to remote ΔK_{th} values of various materials are well comparable to experimentally obtained effective thresholds.

The clear physical background of the dislocation-based model provides technologists with a good tool for improvement of the resistance to fatigue crack propagation by means of microstructure variation.

ACKNOWLEDGEMENT

This work was supported by the Ministry of Education, Youth and Sports of the Czech Republic in the frame of the project MSM0021630518. Valuable discussions with Prof. P. Šandera from the Brno University of Technology are also acknowledged.

REFERENCES

[1] J. Pokluda, P. Šandera, In: A Multiscale Context, Springer-Verlag London Limited, UK (2010).
[2] P. C. Paris, J. Erdogan, J. Basic Eng., 85 (1963) 528.
[3] J. R. Rice, In: Fatigue Crack Propagation, ASTM STP 415, Philadelphia, (1967).
[4] M. N. James, M. N. Pacey, L. W. Wei, E. A. Patterson, Engng. Fract. Mech., 70 (2003) 2473.
[5] M. N. Pacey, M. N. James, E. A. Patterson, Expl. Mech., 45 (2005) 45.
[6] C. J. Christopher, M. N. James, E. A. Patterson, K. F. Tee, Int. J. Fract., 148 (2007) 361.
[7] R. Pippan, G.Strobl, H. Kreuzer, C. Motz, Acta Mater., 52 (2004) 4493.
[8] J. Pokluda, P. Šandera, R. Pippan, In: Fatigue 06, Edited by W. S. Johnson. Elsevier, Atlanta, Georgia, USA (2006) 0107A_03.
[9] J. Pokluda, R. Pippan, Mater. Sci. Eng., A462 (2007) 355.
[10] R. Pippan, Engng. Fract. Mech., 44 (1993) 821.
[11] F. O. Riemelmoser, R. Pippan, O. Kolednik, Comput. Mech., 20 (1997) 139.
[12] F. O. Riemelmoser, R. Pippan, H. P. Stüwe, Acta Mater., 46 (1998) 1793.
[13] S. Suresh, Fatigue of materials. Cambridge University Press, Cambridge, UK (1998).
[14] H. J. Lee, J. H. Song, Fatigue Fract. Engng. Mater. Struct. 28 (2005) 333.
[15] F. V. Antunes, R. Branco, R. M. Rodrigues, Key Engng. Mater., 465 (2011) 548.
[16] J. Pokluda, P. Šandera, J. Horníková, Fat. Fract. Engng. Mater. Struct., 27 (2004) 141.

[17] J. R. Cook, P. E. Irwing, G. S. Both, C. J. Beevers, Engng. Fract. Mech., 7 (1974) 67.
[18] J. Pokluda, J. Siegl, Fat. Fract. Engng. Mater. Struct., 13 (1990) 375.
[19] O. Kolednik, Int. J. Sol. Struct., 37 (2000) 781.
[20] T. Hanlon, S. Suresh, In: International Congress on Fracture (ICF11), Edited by A. Carpinteri, Politecnico di Torino, Torino Italy, (2005) 463.
[21] R. D. Carter, E. W. Lee, E. A. Starke, C. J. Beevers, Metall. Trans., 15A (1984) 555.
[22] R. Pippan, Phil. Mag., 77A (1998) 861.
[23] J. L. Robinson, C. J. Beevers, Metal Sci., 7 (1973) 153.
[24] J. K. Gregory, In: Fatigue and Fracture, Edited by Lampman et al.. ASM Hanbook, , Metals Park, OH, 19 (1996) 845.
[25] B. L. Boyce, R. O. Ritchie, Engng. Fract. Mech., 68 (2001) 129.
[26] R. Pippan, Mater. Sci. Eng., A138 (1991) 1.